High-temperature electron–hole transport in PrBaCo$_2$O$_{5+\delta}$

A.Yu. Suntsov *, I.A. Leonidov, M.V. Patrakeev, V.L. Kozhevnikov

Institute of Solid State Chemistry, Yekaterinburg 620990, Russia

ARTICLE INFO

ABSTRACT

The oxygen content, conductivity and thermopower in the double perovskite-like cobaltite PrBaCo$_2$O$_{5+\delta}$ are reported in the oxygen partial pressure range 2×10^{-6}–0.21 atm and temperatures between 650 and 950 °C. The electrical properties are shown to be continuous through the transition from $\delta > 0.5$ to $\delta < 0.5$. The variations of transport parameters with temperature and oxygen content reveal hole polaron hopping conduction within oxygen non-stoichiometry domain $\delta < 0.5$.

Crown Copyright © 2011 Published by Elsevier Inc. All rights reserved.

1. Introduction

The double perovskite-like cobaltites RBaCo$_2$O$_{5+\delta}$, where R is a rare-earth metal, enter the family of non-stoichiometric oxides where oxygen content variations δ can achieve as much as one oxygen atom per formula unit. The singular point within oxygen homogeneous range is $\delta = 0.5$ where nominal charge of cobalt cations is 3+, and oxygen vacancies are ordered along a-axis so that rows of CoO$_5$ pyramids alternate with rows of CoO$_6$ octahedra [1–7]. The singularities in charge state and structure are accompanied with a peculiar configuration of the phase diagram, unusually large thermopower values in the low-temperature insulating regime and other anomalies at oxygen non-stoichiometry value near $\delta = 0.5$ [8]. In the low temperature range ($T \sim 100$ K), where Co^{3+} cations in CoO$_6$ octahedra are in the low spin $t_{2g}^6 e_g^0$ state and concentration of charge carriers mainly depends on oxygen content, thermopower is positive at $\delta > 0.5$ and negative at $\delta < 0.5$ [5–8]. The thermopower decrease and thermally activated conductivity, which may be observed at higher temperatures in specimens with oxygen "excess" ($\delta > 0.5$) and oxygen "deficiency" ($\delta < 0.5$), are related with formation of electron–hole pairs, or Co^{2+}–Co^{4+} in a localized picture [7,9–11]. It is argued that different motion of electron and hole carriers and predominant hole conductivity are due to suppressed hopping of a high-spin Co^{2+} electron over a low-spin Co^{3+} background because of a spin blockade mechanism at temperatures below the metal–insulator transition [7,9]. The importance of the interplay of charge and spin degrees of freedom was stressed in earlier works on transport properties of

LaCoO$_3$ [12,13]. One should add also that equal concentrations of Co^{2+} and Co^{4+} cations are observed in LaSrCoO$_4$, where cobalt nominal charge is 3+ [14]. However, the oxygen content in LaCoO$_3$ or LaSrCoO$_4$ remains practically invariable in wide limits of temperature and oxygen pressure so that the equilibrium of cobalt species depends only on temperature. At the same time considerable variations of the non-stoichiometry parameter δ may strongly influence the charge equilibrium in RBaCo$_2$O$_{5+\delta}$ [8,15]. Additional interest to transport properties of RBaCo$_2$O$_{5+\delta}$ cobaltites is related to the search of advanced membrane materials for oxygen separation and for SOFC cathodes because complementary to electronic carriers these compounds exhibit at heating high mobility of oxygen ions also [16–18]. The enhancement of the oxygen ion mobility above 400 °C is facilitated by redistribution of oxygen ions over O3 and O4 positions in the orthorhombic structure (e.g. *Pmmm*) [19], and the oxygen diffusion coefficient achieves about 10^{-5} cm^2/s [18] in the disordered tetragonal phase RBaCo$_2$O$_{5+\delta}$ (e.g. *P4/mmm*) near 500 °C [19,20]. On the whole, the understanding of charge states of cobalt cations in the double perovskite-like cobaltites, and particularly at elevated temperatures, seems to be insufficient. Therefore, in this work we have attempted to track the influence of oxygen content variations upon electrical conductivity and thermopower in PrBaCo$_2$O$_{5+\delta}$, where the non-stoichiometry parameter δ can vary in particularly wide limits at relatively small changes of external thermodynamic parameters.

2. Experimental

The samples of PrBaCo$_2$O$_{5+\delta}$ were obtained by solid state synthesis from high purity oxides Pr$_6$O$_{11}$ and Co$_3$O$_4$, and barium carbonate BaCO$_3$. The starting reagents were pretreated by

---

heating in air at appropriate temperatures in order to remove adsorbates. The respective mixture was thoroughly ground with a mortar and pestle, pelletized and calcined in air at 900–1150 °C. The procedure was repeated several times with the gradual increase of the firing temperature. After heating during 24 h at the final stage, the specimens were slowly cooled down to room temperature.

The phase purity control and determination of crystal lattice parameters at room temperature were carried out by powder X-ray diffraction using a STADI-P (STOE) diffractometer. The air synthesized cobaltite $PrBaCo_2O_{5+\delta}$ was confirmed to be a single phase having an orthorhombic structure (e.g. $Pmmm$) with the unit cell parameters $a=3.8981(1)$ Å, $b=7.8069(2)$ Å and $c=7.6345(2)$ Å characteristic of a double perovskite.

The oxygen content in the as-prepared cobaltite was determined with the help of a SETARAM TG-92 thermoanalyzer by reduction in the gas mixture containing 5% of H_2 and 95% of He. Heating in the hydrogen containing atmosphere resulted in the reduction of the cobaltite to BaO and Pr_2O_3 oxides, and cobalt metal. The respective weight loss was utilized in order to calculate oxygen content in the as-prepared material. The oxygen non-stoichiometry parameter $\delta=0.77$ in as-synthesized samples was found to be in agreement with earlier results [15,21]. The equilibrium oxygen content in the cobaltite at different values of temperature (T) and partial pressure of oxygen pO_2 in the gaseous phase was measured by coulometric titration as described elsewhere [22]. The absolute changes of oxygen content in the specimen on heating in air $pO_2=0.21$ atm were determined with the thermoanalyzer, and the value of δ obtained at $T=650$ °C and $pO_2=0.21$ atm was used as a reference point for coulometric titration data.

Rectangular bars $2 \times 2 \times 15$ mm were cut from the sintered pellets for electrical measurements. One specimen, equipped with butt electrodes and thermocouples, was used for measurements of thermopower (α). The temperature gradient in the furnace along the sample was about 20 K/cm. Another specimen was used in four-probe measurements of the d.c. conductivity (σ). Current leads of platinum wire (0.3 mm) were tightly wound to the sample at 14 mm spacing while the spacing between the potential probes was 10 mm. The specimen was placed perpendicular to the specimen for thermopower measurements so that the temperature gradient along the sample was zero. The measurements of conductivity and thermopower were carried out simultaneously in a cell utilizing oxygen sensing and pumping properties of cubically stabilized zirconia oxygen electrolyte as described in [23]. The electrical parameters were measured with a high-precision SOLARTRON 7081 voltmeter. Experimental data points were collected only after equilibrium had been achieved between the sample and ambient oxygen gas, that is when changes in the logarithm of the conductivity did not exceed 0.01% per minute and changes in thermopower did not exceed 0.001 μV/min. The measurements were carried out in isothermal runs. The measurements were halted upon achievement of the desirable low-pressure limit. Then the oxygen pressure was increased to the starting upper limit where measurements were repeated in order to confirm reversibility of the experiment; thereupon temperature was changed thus enabling the next measuring cycle. Thermopower data were corrected for the contribution of the platinum leads [24].

3. Results and discussion

The measured isotherms of electrical conductivity and thermopower versus partial pressure of oxygen are presented in Figs. 1 and 2, respectively. The positive values of thermopower
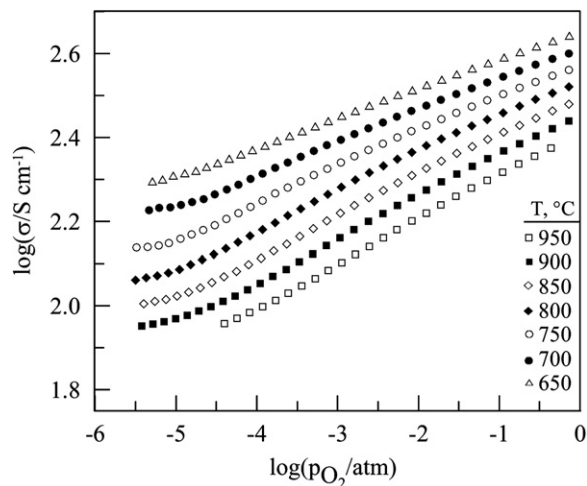

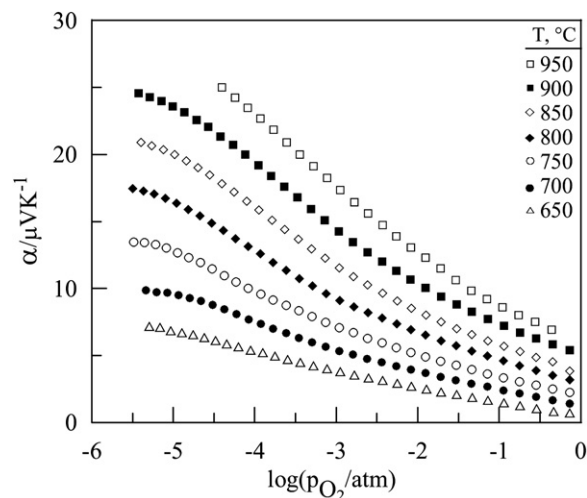**Fig. 1.** Isothermal conductivity in $PrBaCo_2O_{5+\delta}$

Fig. 2. Isothermal thermopower in $PrBaCo_2O_{5+\delta}$

show that electron holes are dominant charge carriers in $PrBaCo_2O_{5+\delta}$ within the entire studied limits of temperature, 650–900 °C, and oxygen partial pressure, 2×10^{-6}–0.21 atm. One can notice additionally that the observed positive slope of the isothermal plots log σ vs. log pO_2 is indicative of p-type majority carriers [20,25,26]. The obtained oxygen content variations at different pressures of oxygen and temperatures (pO_2–T–δ diagram) are shown in Fig. 3. Combining the data in Figs. 1–3, one can plot composition dependent isotherms for σ and α in Figs. 4 and 5, respectively. It is clearly seen that variations of electric properties with temperature at permanent oxygen content are relatively small while oxygen content changes profoundly influence both conductivity and thermopower, which agrees with observations in works [20,25,26]. The non-linear increase of isothermal conductivity

$$\sigma = |e|\mu p, \tag{1}$$

may reflect simultaneous increase of hole mobility, μ, and concentration, p, with oxygen content in $PrBaCo_2O_{5+\delta}$. This behavior is typical for perovskite-like oxides with B-cations in different oxidation states [27–29], where it is attributed to the increase in amount and average length of transport chains $-B^{n+}-O^{2-}-B^{n+1}-$ [30].

The conductivity values at permanent oxygen content exhibit some decrease with the temperature increase that at first glance
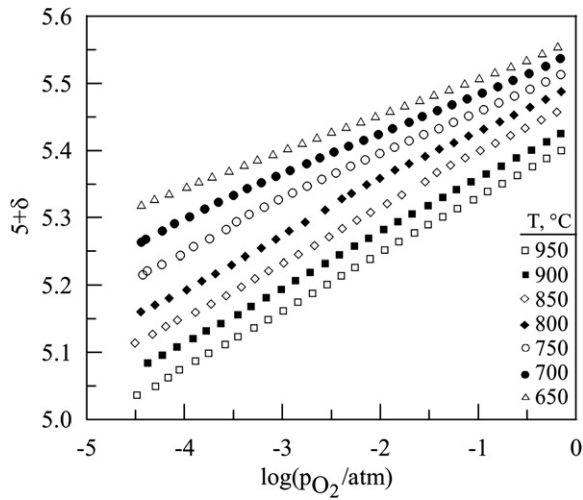
Fig. 3. Oxygen content changes in PrBaCo$_2$O$_{5+\delta}$ at different temperatures.

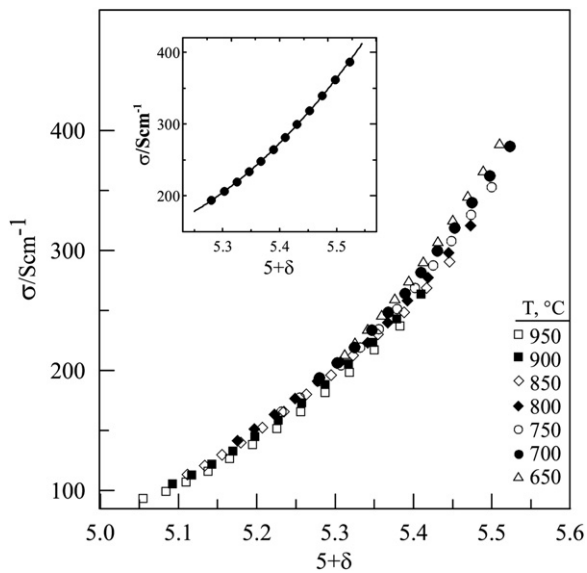**Fig. 6.** Arrhenius plots for conductivity in PrBaCo$_2$O$_{5+\delta}$ at different values of oxygen content.

Fig. 4. Conductivity isotherms vs. oxygen content in PrBaCo$_2$O$_{5+\delta}$. The inset shows the isotherm at 700 °C. The solid line is a guide to the eye.

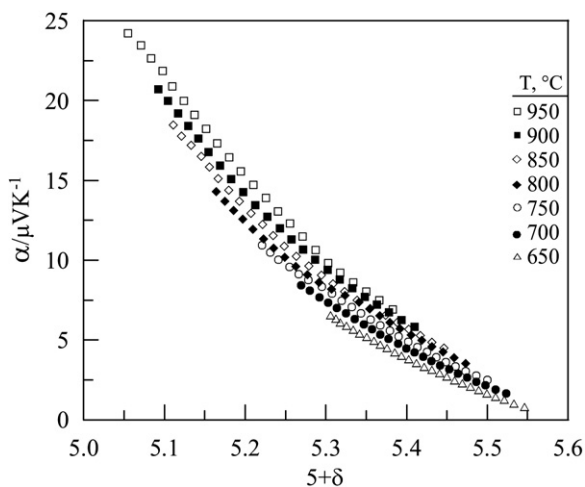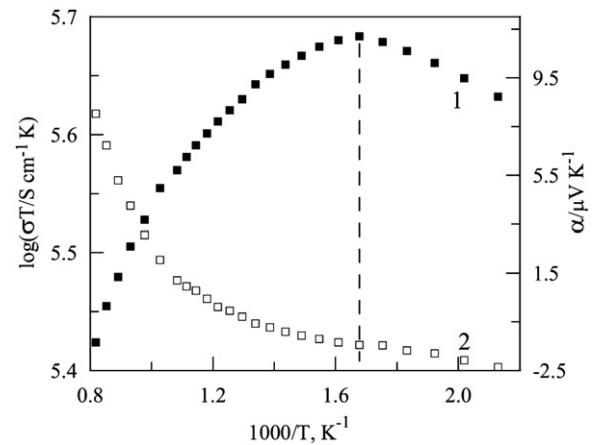**Fig. 7.** Arrhenius plots for conductivity (1) and thermopower (2) in PrBaCo$_2$O$_{5+\delta}$ at heating in air. The oxygen deintercalation temperature is shown by dashed line.

can be interpreted as evidence to metallic-like character of PrBaCo$_2$O$_{5+\delta}$ at elevated temperatures. However, similar changes are not inconsistent with the small polaron conduction mechanism because the prefactor in the adiabatic small polaron mobility $\mu = (\mu_0/T)\exp(-E_a/kT)$ gives rise to the possibility of a conductivity that decreases with increasing temperature in the limit that T is high and E_a is low [19,31]. Indeed, the cross-sections of Fig. 4 at $\delta =$ const enable one to obtain the $\log(\sigma T)$ vs. $1/T$ plots that demonstrate a semi-conductor type high-temperature conductivity in PrBaCo$_2$O$_{5+\delta}$ with the mobility activation energy of about 0.04–0.06 eV independent on oxygen content (Fig. 6). The same activation energy is observed in as-prepared PrBaCo$_2$O$_{5.77}$ at measurements in air below 320 °C (Fig. 7), and in oxygen depleted PrBaCo$_2$O$_{5.5}$ above 100 °C in conditions where there is no oxygen exchange between gaseous phase and the specimen [19]. This observation suggests that the nature of hole carriers at temperatures lower than in the present work, i.e., from 600 down to at least 100 °C, remains essentially the same as in the interval 600–950 °C.

The thermopower of polaron hole carriers in PrBaCo$_2$O$_{5+\delta}$ can be expressed as [32]

$$\alpha = \frac{k}{|e|}\ln\left(\frac{1}{\beta}\frac{N}{p}\right), \qquad (2)$$

Fig. 5. Thermopower isotherms vs. oxygen content in PrBaCo$_2$O$_{5+\delta}$.

where e is the electron charge, N is the concentration of lattice sites available for polaron jumps and β is the spin degeneracy factor. Neglecting the weak temperature dependence, which can be attributed to anion disordering, one can see that the thermopower decrease in Fig. 5 gives evidence to the increase in concentration of holes with oxygen content.

Considering the pO_2–T–δ diagram in Fig. 3 one can notice that oxygen content in the cobaltite at utilized experimental conditions does not exceed $5+\delta=5.5$ in the nearly entire range of measured parameters. Even a slight decrease of oxygen partial pressure results in smaller oxygen content as well as heating above 650 °C, and according to electrical neutrality requirement only Co^{2+} and Co^{3+} cations are supposed to be in equilibrium in $PrBaCo_2O_{5.5}$ at $5+\delta<5.5$. Hence, one can try to consider mobile holes as Co^{3+} cations in localized description, and their movement as related with hops over a Co^{2+} background. In such a case the conductivity must change proportionally to the concentration product $[Co^{3+}][Co^{2+}]$. Because $[Co^{3+}]=(1+2\delta)$ and $[Co^{2+}]=(1-2\delta)$ one can conclude that the conductivity should change with oxygen content proportionally to $(1+2\delta)(1-2\delta)$, which is a decreasing function of δ in evident controversy with experimental data in Fig. 4. One can speculate also that the oxygen distribution over $PrBaCo_2O_{5+\delta}$ is not homogeneous so that there are local regions reach with oxygen ($\delta>0.5$) that provide mobile holes (Co^{4+} cations). However, it is difficult to see the reason for this phenomenon to persist up to about 1000 °C in cobaltites, which are known as compounds with highest oxygen mobility among oxide materials. Moreover, changes of temperature and oxygen pressure ought to influence the average size and connection of the inhomogeneous oxygen clusters that, in turn, would result in a hysteresis of the *in situ* conductivity and thermopower measurements. Such a hysteresis was never observed in the used experimental conditions. On the other hand, thermopower and conductivity isotherms in Figs. 2 and 3, respectively, do not reveal any discontinuity at transition from the range $\delta>0.5$, where holes are identified as Co^{4+} cations [7,31,33], to the range $\delta<0.5$. This smooth behavior suggests that the concentration of holes does not experience any sudden change at $\delta=0.5$, and the hops of mobile holes over Co^{3+} background uphold conduction at $\delta<0.5$.

The formation of Co^{4+} cations at high temperatures can be explained as a result of partial oxidation of Co^{3+} cations:

$$1/2O_2+V_0+2Co^{3+}=O^{2-}+2Co^{4+} \tag{3}$$
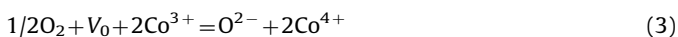
Moreover, thermal equilibrium

$$2Co^{3+}=Co^{2+}+Co^{4+} \tag{4}$$

may influence concentration of different cobalt species [14,31,34]. Assuming simultaneous presence of Co^{2+}, Co^{3+} and Co^{4+} cations, the cobaltite formula can be presented as $PrBaCo_n^{2+}Co_N^{3+}Co_p^{4+}O_{5+\delta}$, where $[Co^{2+}]\equiv n$, $[Co^{3+}]\equiv N$ and $[Co^{4+}]\equiv p$. Taking into account site balance

$$N+n+p=2 \tag{6}$$

and electroneutrality

$$2n+3N+4p=5+2\delta \tag{7}$$

requirements one can see that

$$N+2p=1+2\delta \tag{8}$$

From (2), (6) and (8) it follows that

$$p=(1+2\delta)/(\beta\exp(\alpha e/k)+2), \quad N=1+2\delta-2p, \quad n=2-N-p \tag{9}$$

The spin degeneracy factor can be calculated as

$$\beta=(2S_3+1)/(2S_4+1) \tag{10}$$

where S_3 and S_4 are spins of Co^{3+} and Co^{4+}, respectively. The combined effects of crystal field and intra atomic exchange at finite temperatures result in energetically most favorable low spin $t_{2g}^5e_g^0$ state of Co^{4+} cations with $S_4=1/2$ in the cobaltites [7,9,12]. As to Co^{3+} in $RBaCo_2O_{5+\delta}$, the most common view is that Co^{3+} cations at moderate temperatures above the insulator to metal transition may adopt high spin $t_{2g}^4e_g^2$ state ($S_3=2$) in CoO_6 octahedra and intermediate spin $t_{2g}^5e_g^1$ state ($S_3=1$) in CoO_5 pyramids [6,35]. Notice also that the structural inequivalence of cobalt sites disappears at heating above 500 °C and formation of the tetragonal phase (e.g. $P4/mmm$) where all Co^{3+} cations reside in structurally equivalent oxygen deficient octahedra [19]. One can suppose, therefore, that Co^{3+} cations in $PrBaCo_2O_{5+\delta}$ are most possibly in high-spin state in the used experimental conditions. Hence, the tentative value for the spin degeneracy factor at high temperatures is $\beta=5/2$.

The results calculated from thermopower with the help of relations (9) are shown in Fig. 8. The values for $[Co^{2+}]$, $[Co^{3+}]$ and $[Co^{4+}]$ are practically independent of temperature in the measured limits 650–950 °C and change linearly with oxygen content. The concentration of Co^{4+} cations is rather high in the entire range $0\le\delta\le0.5$. The intrinsic equilibrium $n=p=0.4$ may be observed when $\delta=0.5$. It is noteworthy that the relative amount of two- and four-charged cobalt cations is about the same in $PrBaCo_2O_{5.5}$ as in $LaCoO_3$ [31]. The product $[Co^{3+}]\cdot[Co^{4+}]$, which defines changes of conductivity with oxygen content, is found to increase in a non-linear manner by about 3.5 times with the increase of δ from 0.05 to 0.5, in exact correspondence with the experimentally observed conductivity behavior and values in Fig. 4. Similar calculations with $S_3=1$ do not reproduce experimentally observed trends in conductivity. Accordingly, high-temperature thermopower data are consistent with high spin Co^{3+} and low spin Co^{4+} states. Moreover, the good agreement gives evidence to negligently small contribution of n-type carriers in electron transport. The conclusion can be drawn, therefore, that mobility of n-type carriers is considerably smaller than of p-type. In difference with the low-temperature insulating regime where mobility of electron and hole carriers strongly depends on their spin state [6,7,9,31], the larger mobility of holes than of electrons at high temperatures may be due to larger bond length Co^{2+}–O^{2-} (2.01 Å) compared to Co^{4+}–O^{2-} (1.93 Å) [36]. Moreover, the hole transport occurs in a e_g-like band of electronic states while
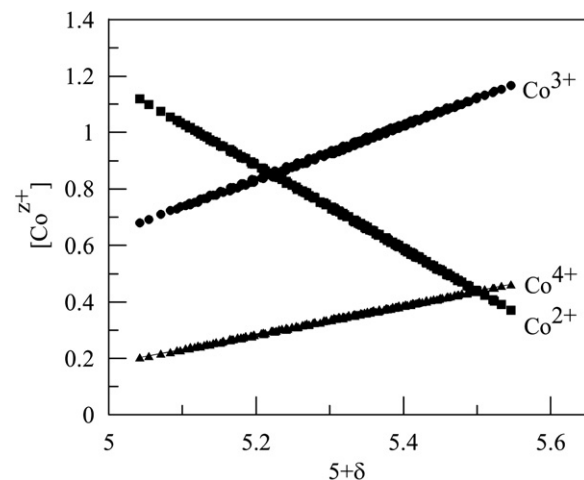

Fig. 8. The calculated concentrations of different cobalt species depending on oxygen content in $PrBaCo_2O_{5+\delta}$ at 650–950 °C.

electron transport over Co^{2+}–O^{2-}–Co^{3+} manifold involves more narrow t_g-like band.

The obtained concentration values can be used in order to evaluate average magnetic moment of cobalt in $PrBaCo_2O_{5.5}$ from

$$\mu_{eff} = \left(\sum_i v_i 4[S_i(S_i+1)] \right)^{1/2} \mu_B, \tag{11}$$

where summation is over three different oxidation states of cobalt, v_i is the fraction of cobalt cations in respective oxidation state, and μ_B is the Bohr magneton. The high-spin Co^{3+} and low spin Co^{4+} values have already been adopted at consideration of thermopower data, and in order to use (11) we need to know the spin state of Co^{2+} cations. Thus, accepting high-spin Co^{2+} cations after [7,9], and utilizing $v_2 = v_4 = 0.2$ and $v_3 = 0.6$ from Fig. 8 one can obtain $\mu_{eff} = 4.2\mu_B$ in $PrBaCo_{0.4}^{2+}Co_{1.2}^{3+}Co_{0.4}^{4+}O_{5.5}$. Though magnetic data for $PrBaCo_2O_{5.5}$ at high temperatures are not available in the literature, one can notice that the calculated result almost exactly coincides with the magnetic moment ($4.3\mu_B$) in the similar cobaltite $GdBaCo_2O_{5.5}$ above the insulator to metal transition [6]. The alternative supposition of low-spin Co^{2+} leads to $\mu_{eff} = 3.9\mu_B$, which is in an inferior correspondence with the available data. From the measured conductivity and calculated concentration values it follows that the hole mobility is about 0.2–0.3 $cm^2\,V^{-1}\,c^{-1}$, which is roughly of the same order of magnitude as the threshold value 0.1 $cm^2\,V^{-1}\,c^{-1}$ that is believed to separate localized and itinerant charge carriers.

4. Conclusion

The oxygen non-stoichiometry, high-temperature conductivity and thermopower of double perovskite-like cobaltite $PrBaCo_2O_{5+\delta}$ were measured from 650 to 950 °C and oxygen partial pressure within 2×10^{-6}–0.21 atm. The continuous change of electric properties with oxygen content variations and positive thermopower exhibit p-type conduction at $\delta \leq 0.5$ as well as at $\delta > 0.5$. The small mobility activation energy and thermopower features support small polaron conduction mechanism in this system. Charge equilibrium of cobalt species that develops simultaneously with the oxygen exchange reaction is shown to play an important role in maintenance of large concentration of holes. The electron-like carriers do not make a viable contribution to conductivity because of their relatively small mobility.

Acknowledgments

References

[1] L. Barbey, N. Nguyen, V. Caignaert, F. Studer, B. Raveau, J. Solid State Chem. 112 (1994) 148–156.
[2] I.O. Troyanchuk, N.V. Kasper, D.D. Khalyavin, H. Szymczak, R. Szymczak, M. Baran, Phys. Rev. Lett. 80 (1998) 3380–3383.
[3] A. Maignan, C. Martin, D. Pelloquin, N. Nguyen, B. Raveau, J. Solid State Chem. 142 (1999) 247–260.
[4] T. Vogt, P.M. Woodward, P. Karen, B.A. Hunter, P. Henning, A.R. Moodenbaugh, Phys. Rev. Lett. 84 (2000) 2969–2972.
[5] D. Akahoshi, Y. Ueda, J. Solid State Chem. 156 (2001) 355–363.
[6] C. Frontera, J.L. García-Muñoz, A. Llobet, M.A.G. Aranda, Phys. Rev. B 65 (2002) 180405(R).
[7] A. Maignan, V. Caignaert, B. Raveau, D. Khomskii, G. Sawatzky, Phys. Rev. Lett. 93 (2004) 026401.
[8] A.A. Taskin, A.N. Lavrov, Y. Ando, Phys. Rev. B 71 (2005) 134414.
[9] A.A. Taskin, Y. Ando, Phys. Rev. Lett. 95 (2005) 176603.
[10] M. Respaud, C. Frontera, J.L. García-Muñoz, M.A.G. Aranda, B. Raquet, J.M. Broto, H. Rakoto, M. Goiran, A Llobet, J. Rodríguez-Carvajal, Phys. Rev. B 64 (2002) 184421.
[11] F. Fauth, E. Suard, V. Caignaert, I. Mirebeau, Phys. Rev. B 65 (2002) 180405 (R).
[12] P.M. Raccah, J.B. Goodenough, Phys. Rev 155 (1967) 932–943.
[13] M.A. Señarís-Rodríguez, J.B. Goodenough, J. Solid State Chem. 116 (1995) 224–231.
[14] T. Matsuura, J. Tabuchi, J. Mizusaki, S. Yamauchi, K. Fueki, J. Phys. Chem. Solids 49 (1988) 1409–1418.
[15] C. Frontera, A. Caneiro, A.E. Carrillo, J. Oro-Sole, J.L. García-Muñoz, Chem. Mater. 17 (2005) 5439–5445.
[16] J-H. Kim, L. Mogni, F. Prado, A. Caneiro, J.A. Alonso, A. Manthiram, J. Electrochem. Soc. 156 (2009) B1376–B1382.
[17] C. Yang, X. Wu, S. Fang, C. Chen, W. Liu, Mater. Lett. 63 (2009) 1007–1009.
[18] A.A. Taskin, A.N. Lavrov, Y. Ando, Appl. Phys. Lett. 86 (2005) 091910.
[19] S. Streule, A. Podlesnyak, D. Sheptyakov, E. Pomjakushina, M. Stingaciu, K. Conder, M Medarde, M.V. Patrakeev, I.A. Leonidov, V.L. Kozhevnikov, J. Mesot, Phys. Rev. B 73 (2006) 094203.
[20] A. Tarancón, D. Marrero-López, J. Peña-Martinez, J.C. Ruiz-Morales, P. Núñez, Solid State Ionics 179 (2008) 611–618.
[21] S. Streule, A. Podlesnyak, J. Mesot, M. Medarde, K. Konder, E. Pomjakushina, E. Mitberg, V. Kozhevnikov, J. Phys.: Condens. Matter 17 (2005) 3317–3324.
[22] E.B. Mitberg, M.V. Patrakeev, A.A. Lakhtin, I.A. Leonidov, V.L. Kozhevnikov, K.R. Poeppelmeier, Solid State Ionics 120 (1999) 239–249.
[23] M.V. Patrakeev, E.B. Mitberg, A.A. Lakhtin, I.A. Leonidov, V.L. Kozhevnikov, V.V. Kharton, M. Avdeev, F.M.B. Marques, J. Solid State Chem. 167 (2002) 203–213.
[24] N. Cusak, P. Kendall, Proc. Phys. Soc. 72 (1958) 898–900.
[25] T.V. Aksenova, L.Y. Gavrilova, A.A. Yaremchenko, V.A. Cherepanov, V.V Kharton, Mater. Res. Bull. 45 (2010) 1288–1292.
[26] D.A. Medvedev, T.A. Zhuravleva, A.A. Murashkina, V.S. Sergeeva, B.D. Antonov, Russ. J. Phys. Chem. A 84 (2010) 1623–1627.
[27] E.B. Mitberg, M.V. Patrakeev, I.A. Leonidov, V.L. Kozhevnikov, K.R. Poeppelmeier, Solid State Ionics 130 (2000) 325–330.
[28] M. Søgaard, P.V. Hendriksen, M. Mogensen, J. Solid State Chem. 180 (2007) 1487–1503.
[29] L. Mogni, J. Fouletier, F. Prado, A. Caneiro, J. Solid State Chem. 178 (2005) 2715–2723.
[30] C. Ziner, Phys. Rev 82 (1951) 403–405.
[31] S.R. Sehlin, H.U. Anderson, D.M. Sparlin, Phys. Rev. B 52 (1995) 11681–11689.
[32] J.P. Doumerc, J. Solid State Chem. 110 (1994) 419–420.
[33] J. Mizusaki, Solid State Ionics 52 (1992) 79–91.
[34] X. Zhang, H. Hao, X. Hu, Physica B 403 (2008) 3406–3409.
[35] Y. Morimoto, T. Akimo, M. Takeo, A. Macida, E. Nisibori, M. Takata, M. Sakata, K Ohoyama, A. Nakamura, Phys. Rev. B 61 (2000) R 13325–R 13328.
[36] R.D. Shannon, Acta Crystallogr. A 32 (1976) 751.